




Surface-enhanced Raman spectroscopy for the quantitative detection of abscisic acid in wheat leaves using silver coated gold nanocomposites

Yanyan Zhang, Hao Zhang, Dongxian Li, Syed Muhammad Zaigham Abbas Naqvi, Mukhtar Iderawumi Abdulraheem, Rui Su, Shakeel Ahmed & Jiandong Hu

To cite this article: Yanyan Zhang, Hao Zhang, Dongxian Li, Syed Muhammad Zaigham Abbas Naqvi, Mukhtar Iderawumi Abdulraheem, Rui Su, Shakeel Ahmed & Jiandong Hu (2021): Surface-enhanced Raman spectroscopy for the quantitative detection of abscisic acid in wheat leaves using silver coated gold nanocomposites, Spectroscopy Letters, DOI: [10.1080/00387010.2021.1995439](https://doi.org/10.1080/00387010.2021.1995439)

To link to this article: <https://doi.org/10.1080/00387010.2021.1995439>

 View supplementary material 

 Published online: 01 Nov 2021.

 Submit your article to this journal 

 View related articles 

 View Crossmark data 



Surface-enhanced Raman spectroscopy for the quantitative detection of abscisic acid in wheat leaves using silver coated gold nanocomposites

Yanyan Zhang^{a,b}, Hao Zhang^{a,b}, Dongxian Li^{a,b}, Syed Muhammad Zaigham Abbas Naqvi^{a,b}, Mukhtar Iderawumi Abdulaheem^{a,b}, Rui Su^{a,b}, Shakeel Ahmed^{a,b} and Jiandong Hu^{a,b,c}

^aCollege of Mechanical and Electrical Engineering, Henan Agricultural University, Zhengzhou, China; ^bHenan International Joint Laboratory of Laser Technology in Agricultural Sciences, Zhengzhou, China; ^cState Key Laboratory of Wheat and Maize Crop Science, Zhengzhou, China

ABSTRACT

A rapid, accurate and novel detection method of plant hormones abscisic acid at ultra-low concentrations in wheat leaves was proposed in this study. This surface-enhanced Raman spectroscopy based method developed the substrate with the silver coated gold nanocomposites. This substrate exhibited excellent detection of rhodamine6G with an ultra-low concentration of 1×10^{-12} M. And resulted in high-performance, well homogeneity and reproducibility against abscisic acid hormone detection with a limit of detection of 1×10^{-9} M. This assay further measured abscisic acid hormones from the fresh leaves extract of wheat with the relative error of 3.72–10.66% compared with enzyme-linked immunosorbent assay bioassay.

ARTICLE HISTORY

Received 6 August 2021
Accepted 10 October 2021

KEYWORDS

Abscisic acid; plant hormone; silver coated gold nanocomposites; surface-enhanced Raman spectroscopy; trace determination

Introduction

Plant hormones such as auxins, gibberellins, cytokinins, abscisic acid (ABA) and ethylene are trace chemical compounds that are synthesized within certain body parts of plants and then transported to the site of action. Although plant hormones occur in plants at low concentration (about 0.038–15.2 nM), they can help the plants to tolerate environmental stress.^[1] Specifically, ABA regulates the physiological responses to environmental stresses such as drought and cold, effectively regulates the vegetative and reproductive growth of plant's root/crown, and significantly improves the quality and yield of crops.^[2] Thus, quantitative detection of the trace concentrations of ABA in the plant is critical to deeply understand the molecular mechanism of plant hormones. A number of measurements have been developed to detect the ABA, where the most widely used approaches include gas chromatography/mass spectrometry (GC/MS),^[3] Electrochemical immunoassay,^[4] Chemiluminescence,^[5] and capillary electrophoresis.^[6] However, these methods are

typically limited to require tedious sample pretreatment and enrichment, as well as expensive instruments in the lab.

Raman spectroscopy is a powerful vibrational spectroscopy technique based on inelastic scattering of light from the molecules of interested.^[7] Raman signal is very weak, its intensity is only 10^{-30} times of incident light, so Raman spectroscopy was not widely used for decades after its discovery in 1928. Until 1977, Van Duyne et al. discovered the surface-enhanced Raman spectroscopy (SERS) effect on roughened silver electrodes, which has become a great breakthrough in Raman spectroscopy.^[8] SERS is capable of identifying specific analyte molecules through their “fingerprint” Raman signals,^[9] where the choice of suitable substrate based on notable metal nanomaterials is important for the improvement of SERS performance. Commonly, SERS substrates with different structures exhibit superior Raman scattering enhancement attributed by both electromagnetic mechanism (EM) and chemical mechanism (CM). EM is mainly induced

by the localized surface plasmon resonance (LSPR) effect,^[10] which is a long term effect with an enhancement factor up to 10^{14} .^[11] CM is derived from the energy exchange between the surrounding molecules and photons driven by the enhanced local electric field,^[12] which is a short-range effect and only happens on the surface of adsorptive metals, and the enhancement factor is generally 10^3 .^[13] Recently, with the merits of high sensitivity, rapid analysis, ultra-low detection limit, trace amount of sample required, excellent reproducibility and partially or completely computerization, SERS has been regarded as a promising and powerful analytical technique in the determination of biological molecules. They have been widely applied in biomedical field,^[14] national defense security,^[15] environmental health,^[16] new energy development^[17] and other fields.^[18] Nevertheless, to the best of our knowledge, the SERS technique has not yet been applied to ABA detection.

In the application of SERS quantitative detection, it is the key that the SERS substrate is simple to fabricate and can generate uniform hot spots.^[19] Both gold (Au) and silver (Ag) nanoparticles are good SERS substrates, the stability of Au is well, while the enhanced effect of Ag is stronger. Therefore, the application of Au and Ag nanocomposites in SERS quantitative detection became more and more extensive, in particular of Au@Ag core-shell structures. He et al. used reporter molecular modified highly monodispersed single-crystal Au nano-spherical particles (AuNSs) as cores to prepare core-shell Au@AgNSs, which exhibited excellent SERS enhancement in the quantitative detection of aflatoxins.^[20] Chen et al. used four kinds of reporter molecules modified between the gold and silver core-shell nanostructures to realize the simultaneous detection of four inflammatory markers.^[21] Most recently, Ag encapsulated Au (Ag@Au) nanospheres were synthesized to obtain higher SERS signals.^[22] In these Au and Ag nanocomposites substrates, internal standard molecules such as 4-Mercaptobenzoic acid (4MBA) are often added between the core and shell to quantify the concentration of analytes. The hidden internal standards can provide stable SERS signal unrelated to the external

environments, laying the foundation for preparing SERS substrates with built-in calibration capacity.

Recently, our group reported a localized surface plasmon resonance (LSPR) sensor to detect ABA in plant hormones and the ideal results were obtained.^[23] However, the development of new plant hormone biosensors is of profound significance for promoting the implementation of rural revitalization plan and food security in China. In this work, the silver coated gold nanocomposites (Au@AgNCs) were synthesized by controlling the deposition of Ag over Au-4MBA seeds using the seed mediated growth method, where the amount of silver nitrate was used to control the thickness of the Ag shell and 4MBA was selected as the internal standard molecule. The morphological and optical properties were characterized by transmission electron microscopy (TEM) image and ultraviolet-visible (UV-Vis) absorption spectra, respectively. Then the Au@AgNCs based SERS substrate was used to quantitatively detect ABA with a concentration range from 1×10^{-9} M to 1×10^{-4} M. This study is the first time to apply SERS technology for the quantitative detection of plant hormone ABA. The research results will provide a certain experimental reference for the development and application of Raman spectroscopy in the detection of plant hormone, and provide a strong research foundation for the later stage research of more sensitive and selective quantitative detection of plant hormone ABA biosensor.

Materials and methods

Materials and instrumentations

Two Tetrachloroauric (III) acid tetrahydrate ($\text{HAuCl}_4 \cdot 4\text{H}_2\text{O}$), Silver nitrate (AgNO_3), L-ascorbic acid (AA) were purchased from Aladdin Reagent Co., Ltd (Shanghai, China). ABA powder, rhodamine6G (R6G, $\text{C}_{28}\text{H}_{30}\text{N}_2\text{O}_3$), 4-mercaptobenzoic acid (4MBA), sodium citrate dihydrate ($\text{C}_6\text{H}_5\text{Na}_3\text{O}_7 \cdot 2\text{H}_2\text{O}$), polyethylene glycol sorbitan monolaurate (Tween20) were purchased from Sigma-Aldrich (USA). Ultrapure water was used for all solution preparations. All glassware used in this research were cleaned using aqua regia

[HCl:HNO₃ = 3:1(v/v)], and rinsed with ultrapure water for several times before experiments.

Ultraviolet-visible spectra were recorded using a UV-Vis spectrophotometer (Nanjing Feiler Instrument Co. LTD, Nanjing, China) with operating wavelength in the range of 300–700 nm. Before measurements, the Au nanoparticles (AuNPs) and core-shell Au@AgNCs colloids were diluted with ultrapure water. Transmission electron microscopy (TEM) images of AuNPs and core-shell Au@AgNCs were obtained using a transmission electron microscope (JEOL JEM-1400 Plus, Tokyo, Japan) operated at an acceleration voltage of 120 kV. The impurities were removed according high speed centrifuge (Hunan Xiangyi Centrifuge Instrument Co. LTD, China), Before centrifugation, all the centrifuge tubes were rinsed with 0.05% TW20 solution to prevent the nanoparticles from adsorbing on the tube wall.

Synthesis of core-shell silver coated gold nanocomposites

Au seeds with an average diameter of about 37 nm were prepared by the reduction of HAuCl₄·4H₂O using trisodium citrate.^[24] In brief, 500 μL of 1% HAuCl₄·4H₂O was added to 49.5 mL ultrapure water in a 100 mL conical flask under slight magnetic stirring. The solution was heated to boiling and kept for 2 min at 120 °C. Then, 1 mL of 1% C₆H₅Na₃O₇·2H₂O was added quickly under vigorous magnetic stirring for 5 min. The colorless solution gradually turns gray, blue, black, and finally gradually stabilizes to purple. The obtained solution was centrifuged at 12,000 rpm for 10 min, and then the sediment was dispersed in the same volume of ultrapure water for further synthesizing core shell Au@AgNCs.

The core shell Au@AgNCs were prepared by a seed mediated growth process.^[25] In brief, 5 μL of 1 mM 4MBA was added to 10 mL of the above AuNPs, magnetically stirred for 20 min, and centrifuged with a speed of 12,000 rpm for 10 min to remove unbound 4MBA, and the sediment was dispersed in the 10 mL ultrapure water. Then, 450 μL of 10 mM AA aqueous solution was added to the tube and mixed with Au-4MBA seeds colloid for 1 min by a magnetic stirrer. Afterwards,

250 μL of 2.5 mM AgNO₃ aqueous solution was added drop by drop to the above solution at a rate of one drop per 3 s upon vigorous shaking. The color of the solution gradually turned from purple to orange with continue stirring for 20 min. For synthesis core shell Au@AgNCs with different thicknesses of Ag shell, keeping the AA level at 450 μL, changing the addition of AgNO₃ ranging from 50 to 300 μL. All the experiments were conducted at 25 °C. The synthetic Au@AgNCs solution needs to be refrigerated at −4 °C in the dark.

Surface-enhanced Raman spectroscopy detection

R6G was used as Raman probe to analyze the SERS sensitivity and reproducibility of the prepared Au@AgNCs SERS substrate. R6G solutions with different levels of concentration were prepared, 100 μL R6G solution (1×10^{-8} – 1×10^{-12} M) was mixed with 400 μL Au@AgNCs colloid and kept for 30 min. Then, 10 μL of the mixture was dropped on the clean silicon wafer and dried at room temperature for SERS detection. The power of incident laser was set to 65 mW. The exposure time was 10 s. Moreover, for detecting ABA using the Au@AgNCs as the SERS active substrate, 50 μL ABA solution (1×10^{-9} – 1×10^{-4} M) was mixed with 50 μL Au@AgNCs colloid, and the SERS signals were also detected on the silicon wafer with the same setting.

The SERS signals were collected by a confocal Raman microscopic system (Pioneer Technology Co. LTD, Beijing, China). The Raman system consists of a high-stable dark-field microscope (BX41, Olympus Co., Center Valley, PA, USA), a confocal Raman module, and a high-resolution spectrometer (Andor Technology Ltd, Belfast, BT127AL, UK) equipped with a CCD (1024 × 256 pixel sensor, Germany). All Raman spectra in this study were collected under a 10× objective with a 532 nm laser radiation.

Real samples

The fresh sample of 0.2 g mature wheat leaves was ground into homogenate with 2 mL extracting solution (containing 80% methanol and 1 mmol/L butylated hydroxytoluene) and

transferred into 10 mL centrifuge tube. Then the mortar was rinsed twice with 3 mL extracting solution, which was then transferred into the centrifuge tube. After shaking, the samples were put into a refrigerator at 4 °C for 6–8 h and centrifuged at 4000 rpm for 10 min to remove the supernatant.^[23] The sediment was dried with N₂ flushing, and the methanol in the extract was removed, then the sample was diluted to 10 mL. The content of wheat hormones ABA was determined by ELISA and SERS.

Results and discussions

The detection principle

The detection principle is the internal standard molecule 4MBA was encapsulated between the gold core and silver shell, and the concentration of internal standard molecule 4MBA is optimized to generate a stable SERS signal. Due to the protection of the silver shell, the internal standard molecules will not be affected by the environmental matrix and will not randomly react with the environmental matrix to affect its SERS signal. The SERS intensity of the mixed solution was detected by mixing different concentrations of ABA solutions with core shell substrate solution containing internal standard molecules that can produce stable SERS signals. As shown in Fig. 1b, 1589 cm⁻¹ is the characteristic Raman peak of 4MBA, and 1637 cm⁻¹ is the characteristic Raman peak of plant hormone ABA. Finally, the relationship between the SERS intensity and ABA concentration was established to achieve quantitative detection of ABA.

Characterization of silver coated gold nanocomposites

It is very important to design noble metal nanoparticles with controllable size and particle morphology to obtain high performance and practical SERS sensing substrates. In this study, four kinds of gold seeds with different diameters were synthesized, and core-shell Au@AgNCs with different shell thickness were synthesized by seed mediated growth method. The morphology of gold cores can be controlled by changing the addition level of trisodium citrate. Fig. S1a–d

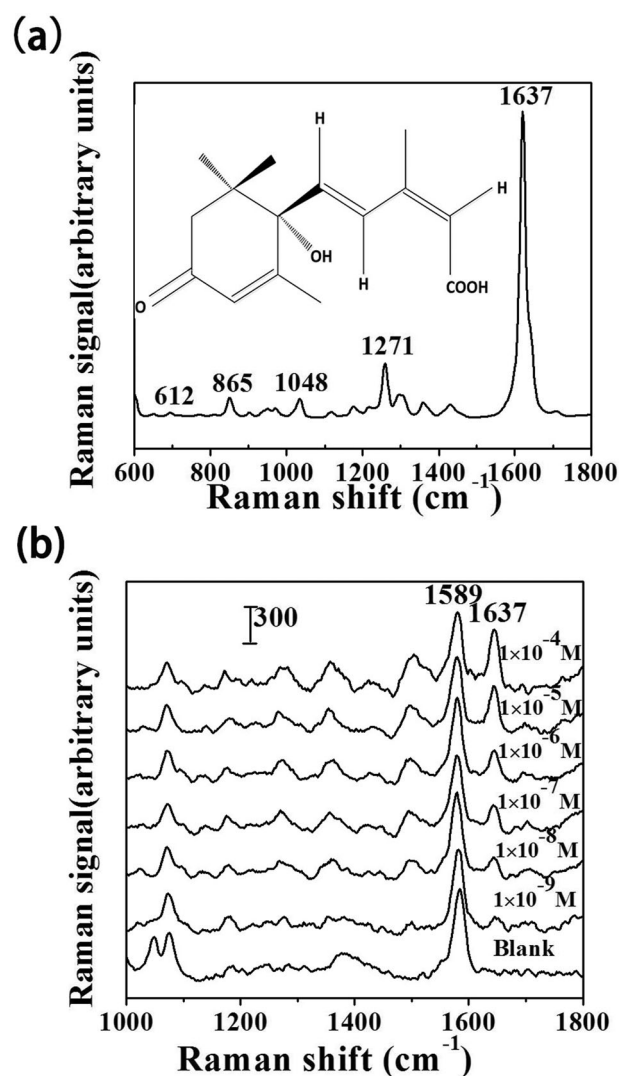


Figure 1. The molecular structure and Raman spectra of abscisic acid powder (a), Surface-enhanced Raman spectroscopy of abscisic acid with different concentrations adsorbed on silver coated gold nanocomposites (b). The detection limit of abscisic acid is 1×10^{-9} M, in the linear range 1×10^{-9} – 1×10^{-4} M, the linear correlation coefficient of abscisic acid is 0.9866.

shows the morphological characteristics of AuNPs formed by adding different doses of 1% trisodium citrate (0.8 mL, 1 mL, 1.2 mL, 1.5 mL) to 50 mL boiled 0.01% H₂AuCl₄·4H₂O. As the dosage of trisodium citrate 1% increased from 0.8 mL to 1 mL, 1.2 mL and 1.5 mL, AuNPs showed spherical morphology and average diameter decreased from about 55 nm to 37 nm, 28 nm and 18 nm, respectively.

The SERS activity of noble metal nanoparticles depends on two competing effects: surface scattering and radiation damping. Surface scattering would affect the imaginary part of the dielectric

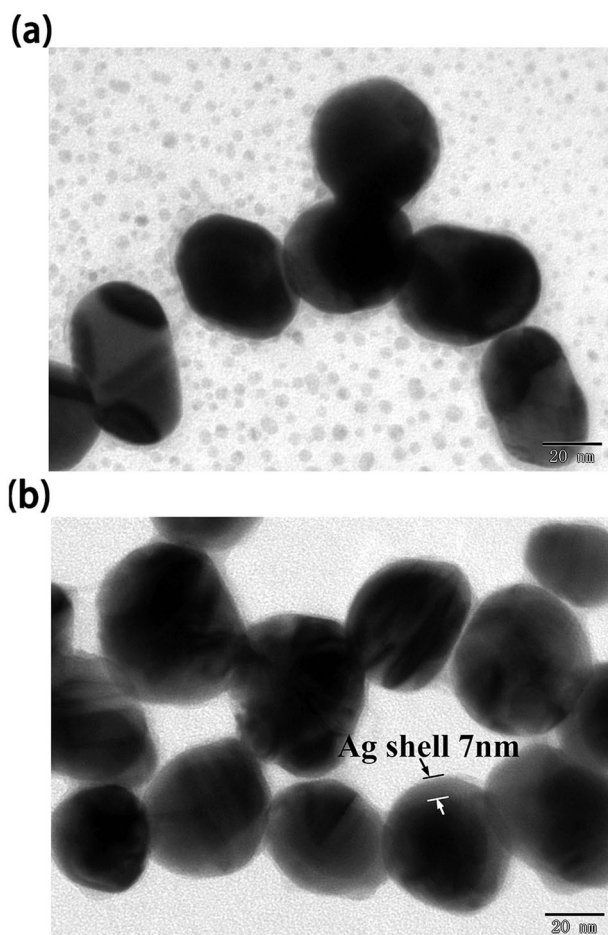


Figure 2. Transmission electron microscopy photos of 37 nm gold nanoparticles (a), the silver coated gold nanocomposites with 37 nm gold core and 7 nm silver shell (b). The photos show the size of the gold core and the thickness of the silver shell.

constant of noble metal, leading drastic changes of surface plasmas, which strongly affected SERS enhancement.^[22] On the one hand, larger nanoparticles can produce stronger enhancement when excited by a laser. On the other hand, as the size of metal nanoparticles increases, the radiation attenuation becomes more severe. Therefore, in this study, 37 nm of intermediate size was taken as the cores to further synthesize core shell nanostructures. As shown in Fig. 2a and Fig. S1c.

The thickness of silver shell certainly affected the sensitivity of silver coated gold nanoparticles as SERS substrate. The lattice constants of gold and silver nanocrystal are very close, just 0.2% apart, so silver can be easily coated on top of gold nanoparticles.^[19] The shell coated core not only protects the nanoparticles from aggregation,

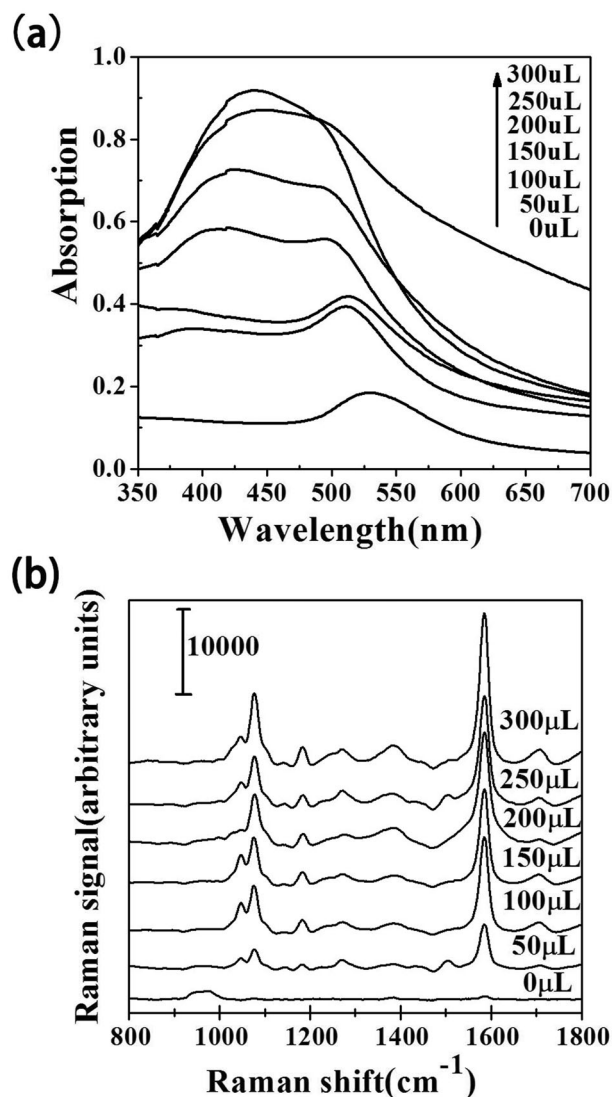


Figure 3. Ultraviolet-visible absorption spectra (a), and Surface-enhanced Raman spectroscopy intensity of the silver coated gold nanocomposites with different volumes of silver nitrate (2.5 mM) and same volumes trisodium citrate (10 mM, 450 μ L) added in gold nanoparticle solution (10 mL) (b). The figure reveal silver shell formation of the silver coated gold nanocomposites.

sintering or other reagents, but also adjusts the sensitivity of core shell nanoparticles by adjusting the thickness of the shell. In order to obtain a strong and stable SERS signal, the amounts of AgNO_3 were optimized to obtain an optimal Ag shell.

The UV-Vis absorption spectra of Au@AgNCs suspensions with different thickness of Ag shell were measured and presented in Fig. 3a. Clearly, when the amount of ascorbic acid was kept as 450 μ L and the amount of AgNO_3 was increased from 50 to 300 μ L, the LSPR peak wavelength of

Ag shell is shifted from 390 nm to 478 nm, indicated the thickness of the silver shell coated on the gold core increased continuously (Fig. S2). Meanwhile, the SERS intensity was greatly affected by the amount of AgNO_3 . As exhibited in Fig. 3b and Fig. S3, the SERS intensity increases with the adding volumes of AgNO_3 from 0 to 300 μL , a relatively high and stable SERS signal is obtained when the volume of AgNO_3 increased to 250 μL , corresponding to a 7 nm thickness of Ag shell (Fig. 2b and Fig. S2e). Although the SERS signal at 300 μL addition of AgNO_3 is slightly stronger than 250 μL (Fig. 3b and Fig. S3), the LSPR peak began to widen as exhibited UV-Vis spectra in Fig. 3a, indicating that there was slight aggregation of silver coated gold nanoparticles, resulting in signal instability, which was owing to the irregular silver shell generation. This result was also confirmed by TEM images of core-shell nanoparticles with different shell thicknesses, as shown in Fig. S2. When the amount of silver nitrate is 50 μL , 100 μL , 150 μL , 200 μL , 250 μL , 300 μL , the corresponding shell thickness is 1 nm, 1.5 nm, 3 nm, 5 nm, 7 nm, 9 nm, respectively. Therefore, the formation of Au@AgNCs with good morphology and the thickness of silver shell can be effectively regulated by adjusting the amount of silver nitrate and ascorbic acid. When the shell thickness exceeds 9 nm, the silver shell covering the surface of gold nanoparticles was too large, resulting in aggregation and precipitation of nanoparticles, as shown in Fig. S2f. Therefore, by taking the SERS activity and stability into account, the Au@AgNCs with Au core diameter of about 37 nm and Ag shell thickness of about 7 nm is chosen as the optimal SERS substrate for further study in our experiments. Fig. S4 shows the average size of the gold core and the average thickness of the silver shell with standard deviation.

Sensitivity and reproducibility of surface-enhanced Raman spectroscopy substrate

With R6G as target molecule, the reproducibility, sensitivity, and the enhanced factor (EF) of the SERS substrate were investigated. As illustrated in Fig. 4a, the Raman characteristic peaks of R6G are located at 1183 cm^{-1} , 1312 cm^{-1} , 1361 cm^{-1} ,

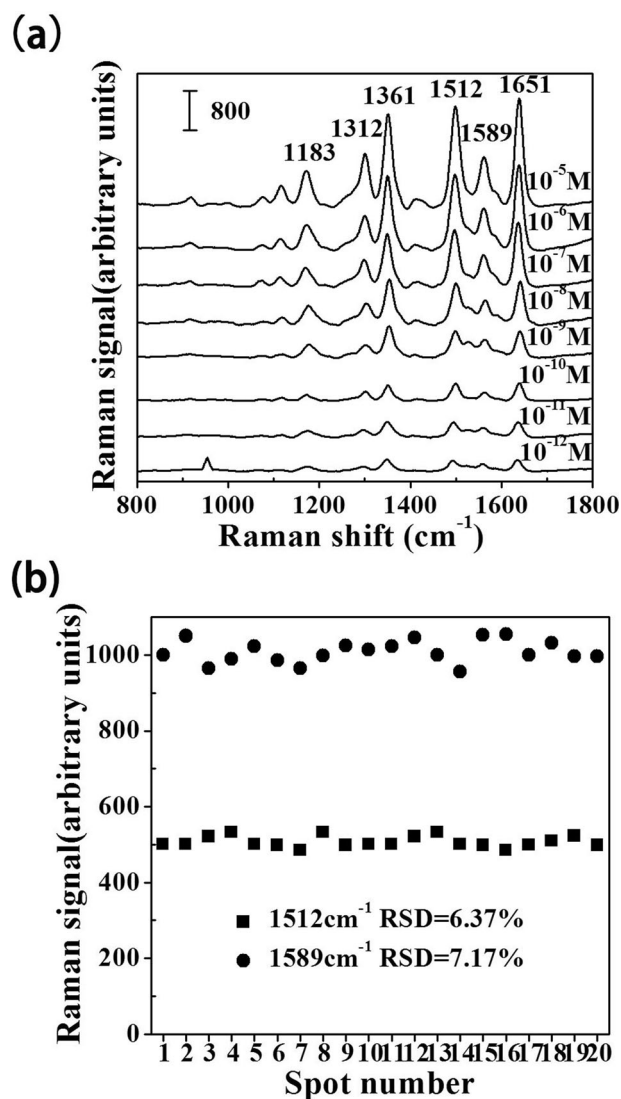


Figure 4. Surface-enhanced Raman signal intensities of Rhodamine 6G with different concentrations absorbed on silver coated gold nanocomposites (a), 20 random Raman signal intensities of Rhodamine 6G with a concentration of 10 nM characteristic peak at 1512 cm^{-1} and 4-mercaptobenzoic acid characteristic peak at 1589 cm^{-1} (b). The figure reveals silver coated gold nanocomposites as Raman substrate have good sensitivity and reproducibility.

1512 cm^{-1} , and 1651 cm^{-1} , while the characteristic peak of 4MBA is 1589 cm^{-1} , the SERS signal of R6G can still be distinctly observed even when the concentration reduces to 10^{-12} M, which indicates an excellent SERS sensitivity of the Au@AgNCs substrate. As shown in Fig. S5, the linear relationship between the SERS intensity of the Raman peak centered at 1512 cm^{-1} and the logarithmic concentration of R6G reveals that, the SERS intensity of R6G has a highly linear correlation ($R^2 = 0.9864$) with its logarithmic concentration.

To further demonstrate the SERS sensitivity of this Au@AgNCs substrate, an approximate EF was estimated. R6G was used to estimate the EF for the silver coated gold nanocomposites. EF is calculated by dividing the SERS intensity normalized by the number of molecules absorbed onto core-shell Au@AgNCs nanostructure to the ordinary Raman intensity normalized by the number of molecules in bulk volume using the following calculation formula (1).^[26] Here, C_{Raman} and C_{SERS} are the concentration of the same volume R6G used for Raman and SERS detection respectively. I_{Raman} and I_{SERS} are the corresponding Raman and SERS signal intensity of R6G with the same volume and different concentrations respectively.

$$EF = \frac{I_{\text{SERS}}/C_{\text{SERS}}}{I_{\text{Raman}}/C_{\text{Raman}}} \quad (1)$$

About 10 μL of 0.1 mM R6G was dropped directly on a silicon wafer for detection for I_{Raman} signal collection. 100 μL R6G solution (10^{-12} M) was mixed with 400 μL Au@AgNCs colloid and kept for 30 min. The final concentration of R6G is 0.2×10^{-12} M. Then, 10 μL of the mixture was dropped on the clean silicon wafer and dried at room temperature for I_{SERS} signal collection. Based on the peak at 1512 cm^{-1} of R6G, I_{Raman} and I_{SERS} were measured to be 184.6 and 214, respectively. The approximate EF was estimated to be 0.58×10^9 , indicating a high SERS sensitivity of the prepared SERS substrate.

In order to evaluate the reproducibility of the Au@AgNCs based SERS active substrate, five batches of Au@AgNCs colloid were prepared and 20 Raman spectra of R6G were randomly collected. The intensity variation of the Raman peak at 1512 cm^{-1} and 1589 cm^{-1} are shown in Fig. 4b. The Raman intensities of the 20 values at 1589 cm^{-1} fluctuated from 978 to 1014, with a relative standard deviation (RSD) value of 7.17%. It has been widely accepted that the reproducibility of a new (or existing) SERS architecture for the quantitative measurement should have RSD less than 20%.^[27] Therefore, the excellent sensitivity and reproducibility provide a great possibility for practical applications of core-shell Au@AgNCs colloid acting as a reliable analytical approach in future.

Optimization of the concentration of 4-mercaptobenzoic acid

The above results indicated that the fabricated SERS substrate can be effectively used to detect R6G. However, the concentration of internal standard molecules 4MBA inevitably affects the performance of the substrate. Therefore, prior to the Ag shell coating, we attempted to optimize the concentration of 4MBA. Six different concentrations of 4MBA ranging from 100 to 600 nM were tested, and the corresponding SERS intensity are shown in Fig. 5a. The SERS signal intensity reaches to a largest value as the concentration of 4MBA increases to 500 nM. Further, the increasing concentration of 4MBA resulting in a declining SERS signal. This phenomenon may be caused by the slight aggregation of nanoparticles due to the increased concentration of ethanol in the dissolved 4MBA.^[21] Thus, 500 nM of 4MBA is chosen as the optimal concentration for modifying the AuNPs core.

To further illustrate the SERS enhanced performance of the substrate and the optimal concentration of the 4MBA, the same concentrations of 4MBA ranging from 100 to 600 nM were modified on Au-4MBA cores, and then Au-4MBA NPs were coated with Ag shells with the same thickness of 7 nm. The corresponding SERS intensity are shown in Fig. 5a, it can be clearly seen from Fig. 5a that the optimized concentration of 4MBA is still 500 nM, where the SERS signal is the largest. Furthermore, it should be noticed that from Fig. 5b the SERS intensity of Au-4MBA@Ag substrate improves almost 10 times when compared to Au-4MBA substrate, This result was consistent with the calculation of EF using R6G molecule as probes, which indicated that the synthesized core-shell Au@AgNCs as SERS substrate have strong enhancement.

Abcisic acid detection using silver coated gold nanocomposites substrate

Fig. 1a displays Raman characteristic peak of ABA powder and the molecular structure of ABA. There are several evident Raman peaks of ABA powder, where the Raman peak at 1637 cm^{-1} is mainly due to stretching vibration of carbon-carbon double bond, the 1271 cm^{-1} peak is assigned to stretching

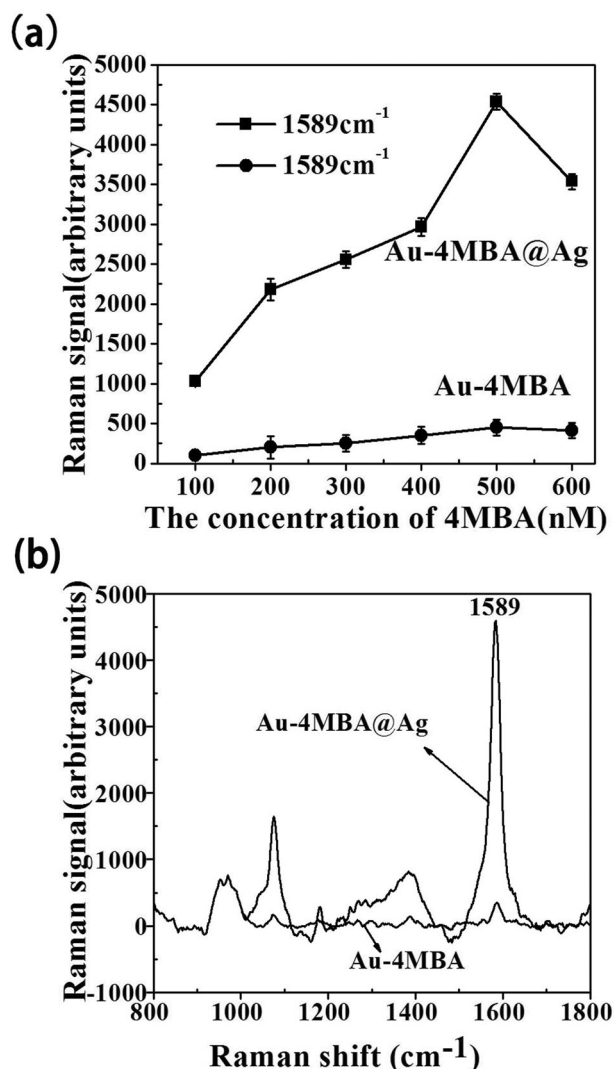


Figure 5. Surface-enhanced Raman signal intensities different concentrations of 4-mercaptobenzoic acid modified on gold core, and between gold core and silver shell (a), comparison of Raman signal intensity of 4-mercaptobenzoic acid characteristic peak at 1589 cm^{-1} before and after formed the silver shell (b). A stable internal standard signal has been obtained by optimizing the concentration of the reporter molecule 4-mercaptobenzoic acid. The volume of 4-mercaptobenzoic acid (1 mM , $5\text{ }\mu\text{L}$) was selected as optimal reporter molecule according to Raman intensities at 1589 cm^{-1} before and after formed the silver shell.

vibration of carbon-carbon single bond. Also the 1048 cm^{-1} is assigned to non-planar oscillation of methyl and the 865 cm^{-1} peak is assigned to torsional vibration of a carbon-carbon single bond, and the 612 cm^{-1} peak is assigned to planar and non-planar oscillations of C-H bonds. Fig. 1b displays the SERS spectra of ABA with different concentrations using Au@AgNCs as substrate. Clearly, the SERS intensity of the characteristic peaks from ABA decreased simultaneously with the reduced concentration of ABA. It can be observed that the

Raman bands are still noticeable even when ABA concentration is as low as $1 \times 10^{-9}\text{ M}$. Thus, the LOD of ABA detected by SERS is $1 \times 10^{-9}\text{ M}$. Because the SERS intensity of the peak at 1637 cm^{-1} is stronger than that of other peaks, this peak was selected to establish the calibration curve between SERS intensity and the ABA concentration. Fig. S6 shows the linear relationship between the SERS intensity of 1637 cm^{-1} and the ABA concentration in logarithmic scale. The fitted equation is $y = 102\lg C + 1004$ with a determination coefficient (R^2) of 0.9866. Furthermore, 5 batches of ABA samples of the same volume were prepared and 20 Raman spectra were randomly collected. The intensity variation of the Raman peak at 1589 cm^{-1} and 1637 cm^{-1} are shown in Fig. S7. The SERS intensities of the 20 values at 1637 cm^{-1} fluctuated from 489 to 510, with a relative standard deviation (RSD) value of 6.33%. This result suggested that it is feasible to utilize Au@AgNCs as the SERS active substrate for detecting trace amounts of plant hormone ABA.

Furthermore, Compared with other ABA detection methods previously reported (Table 1), the detection of ABA using silver coated gold nanocomposites as SERS substrate had a wider linear range and a relatively low LOD, and the linear range was wider than that of chromatography detection of ABA, and the detection speed was faster. Once the silver coated gold nanoparticles were synthesized, they can be used for a long period of time, and the testing time is only a few seconds. The detect method is simple to operate and does not require the participation of professionals, which is suitable for farmers to monitor the changes of plant hormones in crops at different growth stages at any time.

Quantification of abscisic acid in real samples and comparison to enzyme-linked immunosorbent assay

To further validate this proposed SERS method in practical applications, fresh leaves of wheat in the mature period were chosen for this experiment. For comparison, the ABA content of these samples was also measured by using ELISA method. The results measured by SERS and ELISA are shown in Table 2. When compared the ELISA method with SERS, the calculated

Table 1. Comparison of the detection results of the developed method with some existing methods for abscisic acid detection.

| Number | Method | Detection range | LOD | References |
|--------|-----------------------------|--------------------|------------------|------------|
| 1 | Capillary electrophoresis | 0.1–10 μ M | 0.28 nM | [6] |
| 2 | Electrochemical immunoassay | 0.01–50 μ g/mL | 0.003 μ g/mL | [4] |
| 3 | Chemiluminescence | 1 pM–10 nM | 1 pM | [5] |
| 4 | Chromatography | 0.2–20 ng/mL | 0.1 ng/mL | [3] |
| 5 | Colorimetric | 5 nM–10 μ M | 2.2 nM | [28] |
| 6 | LSPR | 0.1 nM–1 mM | 0.51 nM | [23] |
| 7 | SERS | 1 nM–100 μ M | 1 nM | This work |

SERS: Surface-enhanced Raman spectroscopy; LSPR: local surface plasmon resonance.

Table 2. Comparison of experimental results between surface-enhanced Raman spectroscopy and enzyme-linked immunosorbent assay of abscisic acid in fresh leaves of wheat ($n = 3$).

| Sample | SERS (nmol/L) | ELISA (nmol/L) | Relative error (%) |
|--------|---------------|----------------|--------------------|
| 1 | 9.9321 | 9.5214 | 4.31 |
| 2 | 10.3165 | 9.9466 | 3.72 |
| 3 | 11.0236 | 10.5632 | 4.36 |
| 4 | 12.8632 | 11.6241 | 10.66 |
| 5 | 13.1268 | 12.1655 | 7.90 |

SERS: Surface-enhanced Raman spectroscopy; ELISA: enzyme-linked immunosorbent assay.

maximum relative error of ABA content is 10.66%, which exhibits an acceptable agreement between these two methods. From the experimental results, it can be concluded that this proposed method could provide a great potential for the detection of ABA and other plant hormones such as ethylene, salicylic acid and so on.

Conclusion

Gold and silver core-shell nanocomposites were synthesized. The SERS enhancement of the Au@AgNCs was quantified by 4MBAs as the Raman reporter molecules. By optimizing the concentration of 4MBA solution and the thickness of silver shell, the Raman activity of SERS substrate was stabilized. Furthermore, R6G was used as Raman probe molecule to test the sensitivity and reproducibility of optimal Au@AgNCs substrate. In this work, this optimal Au@AgNCs substrate has been shown for the first time to be successfully used for the detection of the plant hormone ABA in a matter of seconds without the need for complex and expensive instruments. This study also demonstrates that the obtained experimental results show a good linear relationship between the SERS intensity and the ABA in the concentration range of 1×10^{-4} – 1×10^{-9} M with a detection limit of 1 nM. The practical use of this assay has been demonstrated by its application to detect ABA from

fresh leaves of wheat with the relative error of 3.72–10.66% when compared with ELISA bioassay. Thus, such measurements have the potential to be readily applied to the detection of other plant hormones such as ethylene and salicylic acid in the future.

Funding

This work was supported by a National Key Research and Development Program of China [2017YFD0801204], the National Natural Science Foundation of China (NSFC) [31671581], the Natural Science Foundation of Henan Province [162300410143].

References

- Buttò, V.; Deslauriers, A.; Rossi, S.; Rozenberg, P.; Shishov, V.; Morin, H. The Role of Plant Hormones in Tree-Ring Formation. *Trees* **2020**, *34*(2), 315–335. DOI: [10.1007/s00468-019-01940-4](https://doi.org/10.1007/s00468-019-01940-4).
- Huang, X. Z.; Hou, L. Y.; Meng, J. J.; You, H. W.; Li, Z.; Gong, Z. Z.; Yang, S. H.; Shi, Y. T. The Antagonistic Action of Abscisic Acid and Cytokinin Signaling Mediates Drought Stress Response in Arabidopsis. *Molecular Plant* **2018**, *11*(7), 970–982. DOI: [10.1016/j.molp.2018.05.001](https://doi.org/10.1016/j.molp.2018.05.001).
- Lu, Q. M.; Zhang, W. M.; Gao, J.; Lu, M. H.; Zhang, L.; Li, J. R. Simultaneous Determination of Plant Hormones in Peach Based on Dispersive Liquid-Liquid Microextraction Coupled with Liquid Chromatography-Ion Trap Mass Spectrometry. *Journal of Chromatography. B Analytical Technologies in the Biomedical and Life Sciences* **2015**, *992*, 8–13. DOI: [10.1016/j.jchromb.2015.04.014](https://doi.org/10.1016/j.jchromb.2015.04.014).
- Bosco, R.; Caser, M.; Vanara, F.; Scariot, V. Development of a rapid LC-DAD/FLD method for the simultaneous determination of auxins and abscisic acid in plant extracts. *Journal of Agricultural and Food Chemistry* **2013**, *61*(46), 10940–10947. DOI: [10.1021/jf4034305](https://doi.org/10.1021/jf4034305).
- Prado, M. J.; Largo, A.; Dominguez, C.; Gonzalez, M. V.; Rey, M.; Centeno, M. L. Immuno Magnetic Assay Combined with CdSe/ZnS Amplification of

- Chemiluminescence for the Detection of Abscisic Acid. *Science China Chemistry* **2011**, *54*(8), 1298–1130. DOI: [10.1007/s11426-011-4326-7](https://doi.org/10.1007/s11426-011-4326-7).
- [6] Liu, X.; Ma, L.; Lin, Y. W.; Lu, Y. T. Determination of Abscisic Acid by Capillary Electrophoresis with Laser-Induced Fluorescence Detection. *Journal of Chromatography. A* **2003**, *1021*(1–2), 209–213. DOI: [10.1016/j.chroma.2003.09.004](https://doi.org/10.1016/j.chroma.2003.09.004).
- [7] Moskovits, M. Surface Roughness and the Enhanced Intensity of Raman Scattering by Molecules Adsorbed on Metals. *The Journal of Chemical Physics* **1978**, *69*(9), 4159–4161. DOI: [10.1063/1.437095](https://doi.org/10.1063/1.437095).
- [8] Fleischmann, M.; Hendra, P. J.; McQuillan, A. J. Raman Spectra of Pyridine Adsorbed at a Silver Electrode. *Chemical Physics Letters* **1974**, *26*(2), 163–166. DOI: [10.1016/0009-2614\(74\)85388-1](https://doi.org/10.1016/0009-2614(74)85388-1).
- [9] Koglin, E.; Sequaris, J. M.; Valenta, P. Surface Raman Spectra of Nucleic Acid Components Adsorbed at a Silver Electrode. *Journal of Molecular Structure* **1980**, *60*, 421–425. DOI: [10.1016/0022-2860\(80\)80102-5](https://doi.org/10.1016/0022-2860(80)80102-5).
- [10] Nie, S. M.; Emory, S. R. Probing Single Molecules and Single Nanoparticles by Surface-Enhanced Raman Scattering. *Science (New York, N.Y.)* **1997**, *275*(5303), 1102–1106. doi:[10.1126/science.275.5303.1102](https://doi.org/10.1126/science.275.5303.1102).
- [11] Moskovits, M. How the Localized Surface Plasmon Became Linked with Surface-Enhanced Raman Spectroscopy. *Notes and Records of the Royal Society* **2012**, *66*(2), 195–203. DOI: [10.1098/rsnr.2011.0024](https://doi.org/10.1098/rsnr.2011.0024).
- [12] Cong, S.; Liu, X. H.; Jiang, Y. X.; Zhang, W.; Zhao, Z. G. Surface Enhanced Raman Scattering Revealed by Interfacial Charge-Transfer Transitions. *Innovation* **2020**, *1*(3), 100051. DOI: [10.1016/j.xinn.2020.100051](https://doi.org/10.1016/j.xinn.2020.100051).
- [13] Sanchez, G. Coupling, Resonance Transmission, and Tunneling of Surface-plasmon Polaritons Through Metallic Gratings of Finite Length. *Physical Review B* **1996**, *53*(15), 10317–10327.
- [14] Peng, Y. J.; Liu, M. H.; Chen, X. F.; Yuan, H. C.; Zhao, J. H. Surface-Enhanced Raman Spectroscopy Coupled with Gold Nanoparticles for Rapid Detection of Amoxicillin Residues in Duck Meat. *Spectroscopy Letters* **2017**, *50*(10), 579–584. DOI: [10.1080/00387010.2017.1397029](https://doi.org/10.1080/00387010.2017.1397029).
- [15] Liu, J. K.; White, I.; DeVoe, D. L. Nanoparticle-Functionalized Porous Polymer Monolith Detection Elements for Surface-Enhanced Raman Scattering. *Analytical Chemistry* **2011**, *83*(6), 2119–2124. DOI: [10.1021/ac102932d](https://doi.org/10.1021/ac102932d).
- [16] Makam, P.; Shilpa, R.; Kandjani, A. E.; Periasamy, S. R.; Sabri, Y. M.; Madhu, C.; Bhargava, S. K.; Govindaraju, T. SERS and Fluorescence-Based Ultrasensitive Detection of Mercury in Water. *Biosensors & Bioelectronics* **2018**, *100*, 556–564. DOI: [10.1016/j.bios.2017.09.051](https://doi.org/10.1016/j.bios.2017.09.051).
- [17] Dong, J. N.; Huang, J. Y.; Wang, A.; Biesold-McGee, G. V.; Zhang, X. N.; Gao, S. W.; Wang, S. C.; Lai, Y. K.; Lin, Z. Q. Vertically-Aligned Pt-Decorated MoS₂ Nanosheets Coated on TiO₂ Nanotube Arrays Enable High-Efficiency Solar-Light Energy Utilization for Photo Catalysis and Self-Cleaning SERS Devices. *Nano Energy* **2020**, *71*, 104579. DOI: [10.1016/j.nanoen.2020.104579](https://doi.org/10.1016/j.nanoen.2020.104579).
- [18] Ogundare, S. A.; van Zyl, W. E. A Review of Cellulose-Based Substrates for SERS: Fundamentals, Design Principles, Applications. *Cellulose* **2019**, *26*(11), 6489–6528. DOI: [10.1007/s10570-019-02580-0](https://doi.org/10.1007/s10570-019-02580-0).
- [19] Li, J. F.; Zhang, Y. J.; Ding, S. Y.; Panneerselvam, Y. R.; Tian, Z. Q. Core-Shell Nanoparticle-Enhanced Raman Spectroscopy. *Chemical Reviews* **2017**, *117*(7), 5002–5069. DOI: [10.1021/acs.chemrev.6b00596](https://doi.org/10.1021/acs.chemrev.6b00596).
- [20] He, H.; Sun, D.-W.; Pu, H.; Huang, L. Bridging Fe₃O₄@Au nanoflowers and Au@Ag nanospheres with aptamer for ultrasensitive SERS detection of aflatoxin B₁. *Food Chemistry* **2020**, *324*, 126832 doi: [10.1016/j.foodchem.2020.126832](https://doi.org/10.1016/j.foodchem.2020.126832).
- [21] Chen, R. P.; Du, X.; Cui, Y. J.; Zhang, X. Y.; Ge, Q. Y.; Dong, J.; Zhao, X. W. Vertical Flow Assay for Inflammatory Biomarkers Based on Nanofluidic Channel Array and SERS Nanotags. *Small* **2020**, *16*(32), 2002801. DOI: [10.1002/sml.202002801](https://doi.org/10.1002/sml.202002801).
- [22] Wang, K. Q.; Sun, D. W.; Pu, H. B.; Wei, Q. Y. Shell Thickness-Dependent Au@Ag Nanoparticles Aggregates for High-Performance SERS Applications. *Talanta* **2019**, *195*, 506–515. DOI: [10.1016/j.talanta.2018.11.057](https://doi.org/10.1016/j.talanta.2018.11.057).
- [23] Wang, S.; Li, W.; Chang, K. K.; Liu, J.; Guo, Q. Q.; Sun, H. F.; Jiang, M.; Zhang, H.; Chen, J.; Hu, J. D. Localized Surface Plasmon Resonance-Based Abscisic Acid Biosensor Using Aptamer-Functionalized Gold Nanoparticles. *Plos One* **2017**, *12*(9), e0185530–13. DOI: [10.1371/journal.pone.0185530](https://doi.org/10.1371/journal.pone.0185530).
- [24] Frens, G. Controlled Nucleation for the Regulation of the Particle Size in Monodisperse Gold Suspensions. *Nature Physical Science* **1973**, *241*(105), 20–22. DOI: [10.1038/physci241020a0](https://doi.org/10.1038/physci241020a0).
- [25] Khlebtsov, N. G. Determination of Size and Concentration of Gold Nanoparticles from Extinction Spectra. *Analytical Chemistry* **2008**, *80*(17), 6620–6625. DOI: [10.1021/ac800834n](https://doi.org/10.1021/ac800834n).
- [26] Hassan, M. M.; Jiao, T. H.; Ahmad, W.; Yi, X.; Zareef, M.; Ali, S.; Li, H. H.; Chen, Q. S. Cellulose Paper-Based SERS Sensor for Sensitive Detection of 2,4-D Residue Levels in Tea Coupled Uninformative Variable Elimination-Partial Least Squares. *Spectrochimica Acta Part A: Molecular and Biomolecular Spectroscopy* **2021**, *248*, 119198. DOI: [10.1016/j.saa.2020.119198](https://doi.org/10.1016/j.saa.2020.119198).
- [27] Natan, M. J. Concluding Remarks: Surface Enhanced Raman Scattering. *Faraday Discussions* **2006**, *132*, 321–328. DOI: [10.1039/b601494c](https://doi.org/10.1039/b601494c).
- [28] Zhou, G. H.; Liu, Y. Z.; Luo, M.; Xu, Q.F.; Ji, X.H.; He, Z. K. Peptide-Capped Gold Nanoparticle for Colorimetric Immunoassay of Conjugated Abscisic Acid. *ACS Applied Materials & Interfaces* **2012**, *4*(9), 5010–5015. DOI: [10.1021/am301380q](https://doi.org/10.1021/am301380q).